# STAT-3 contributes to pulmonary fibrosis through epithelial injury and fibroblast-myofibroblast differentiation

**Mesias Pedroza,* Thuy T. Le,† Katherine Lewis,‡ Harry Karmouty-Quintana,† Sarah To,* Anuh T. George,* Michael R. Blackburn,† David J. Tweardy,‡ and Sandeep K. Agarwal*,[1]**

*Department of Medicine and ‡Department of Infectious Disease, Baylor College of Medicine, Houston, Texas, USA; and †Department of Biochemistry and Molecular Biology, University of Texas Health Science Center, Houston Medical School, Houston, Texas, USA

ABSTRACT **Lung fibrosis is the hallmark of the interstitial lung diseases. Alveolar epithelial cell (AEC) injury is a key step that contributes to a profibrotic microenvironment. Fibroblasts and myofibroblasts subsequently accumulate and deposit excessive extracellular matrix. In addition to TGF-β, the IL-6 family of cytokines, which signal through STAT-3, may also contribute to lung fibrosis. In the current manuscript, the extent to which STAT-3 inhibition decreases lung fibrosis is investigated. Phosphorylated STAT-3 was elevated in lung biopsies from patients with idiopathic pulmonary fibrosis and bleomycin (BLM)-induced fibrotic murine lungs. C-188-9, a small molecule STAT-3 inhibitor, decreased pulmonary fibrosis in the intraperitoneal BLM model as assessed by arterial oxygen saturation (control, 84.4 ± 1.3%; C-188-9, 94.4 ± 0.8%), histology (Ashcroft score: untreated, 5.4 ± 0.25; C-188-9, 3.3 ± 0.14), and attenuated fibrotic markers such as diminished α–smooth muscle actin, reduced collagen deposition. In addition, C-188-9 decreased the expression of epithelial injury markers, including hypoxia-inducible factor-1α (HIF-1α) and plasminogen activator inhibitor-1 (PAI-1). *In vitro* studies show that inhibition of STAT-3 decreased IL-6– and TGF-β–induced expression of multiple genes, including HIF-1α and PAI-1, in AECs. Furthermore, C-188-9 decreased fibroblast-to-myofibroblast differentiation. Finally, TGF-β stimulation of lung fibroblasts resulted in SMAD2/SMAD3-dependent phosphorylation of STAT-3. These findings demonstrate that STAT-3 contributes to the development of lung fibrosis and suggest that STAT-3 may be a therapeutic target in pulmonary fibrosis.—Pedroza, M., Le, T. T., Lewis, K., Karmouty-Quintana, H., To, S., George, A. T., Blackburn, M. R., Tweardy, D. J., Agarwal, S. K. STAT-3 contributes to pulmonary fibrosis through epithelial injury and fibroblast-myofibroblast differentiation. *FASEB J.* 30, 129–140 (2016). www.fasebj.org**

*Key Words: fibrosis · STAT3 · epithelial injury · myofibroblast*

Interstitial lung diseases (ILDs), also known as diffuse parenchymal lung diseases, are a group of heterogeneous lung disorders characterized by varying degrees of inflammation and extracellular matrix (ECM) remodeling in the lung parenchyma and alveolar space (1, 2). Idiopathic pulmonary fibrosis (IPF) is the most common of these disorders. The prevalence of IPF has been reported as high as 63 cases per 100,000, and incidence rates are increasing (3–5). Age-adjusted and standardized mortality rates from IPF are also increasing (6). Treatment options for IPF remain limited. Understanding the pathogenesis of ILD continues to be an unmet need and a critical step in the development of potential therapeutic targets.

Pulmonary fibrosis is the hallmark of ILDs and represents a final common pathway of these lung disorders. Current paradigms point to alveolar epithelial cell (AEC) injury as a critical step in the pathogenesis of lung fibrosis. Injured type II AECs lead to dysregulated activation and create a profibrotic microenvironment including persistently activated wound repair pathways (7, 8). The result is the formation of fibroblastic foci that contain increased numbers of fibroblasts and myofibroblasts that deposit large amounts of ECM and destroy the normal alveolar architecture (9–15). TGF-β is a central mediator of fibrosis and an important driver of myofibroblast differentiation and activation, but other cytokines including IL-6 have also been suggested to play key roles (16–18).

IL-6 is a member of the IL-6 family of cytokines that shares a common receptor signal transduction molecule called gp130. Upon activation of gp130, IL-6 family cytokines trigger activation of Janus kinases and eventually STAT-3, a latent cytoplasmic transcription factor. Given the shared signaling, members of the IL-6 family also may display overlapping biologic activities. IL-6 elicits multiple responses, both proinflammatory and profibrotic, depending on the context within which it is expressed. IL-6 is elevated in the serum of patients with

Abbreviations: α-SMA, α-smooth muscle actin; AEC, alveolar epithelial cell; BAL, bronchoalveolar lavage; BLM, bleomycin; Col1α1, collagen 1α1; ECM, extracellular matrix; FEV1, forced expiratory volume in 1 s; FSP-1, fibroblast specific protein 1; FVC, forced vital capacity; GAPDH, glyceraldehyde 3-phosphate dehydrogenase; H&E, hematoxylin and eosin;

(*continued on next page*)

[1] Correspondence: Department of Medicine, Section of Immunology, Allergy and Rheumatology, Department of Pathology and Immunology, Biology of Inflammation Center, One Baylor Plaza, Suite 672E, M.S.: BCM285, Houston, TX 77030, USA. E-mail: skagarwa@bcm.edu

doi: 10.1096/fj.15-273953

This article includes supplemental data. Please visit *http://www.fasebj.org* to obtain this information.

systemic sclerosis (19), lungs of patients with IPF (20), and in mouse models of pulmonary fibrosis (16, 17). Targeting IL-6 *via* genetic deletion or IL-6–neutralizing antibodies reduces pulmonary fibrosis (17). Downstream targeting of IL-6 and IL-6 family members *via* STAT-3 inhibition may represent an alternative approach to the treatment of fibrosis.

The role of STAT-3 in fibrosis has not been fully defined, and studies have yielded conflicting results depending on the tissues involved (21–26). With regard to lung fibrosis, levels of phosphorylated STAT-3 (phospho-STAT-3) have been shown to be elevated in patients with IPF and the intratracheal bleomycin (ITB) model (18, 27–29). One study demonstrated that STAT-3 haploinsufficiency (STAT-$3^{+/-}$) protected mice from the development of lung fibrosis in the ITB but did investigate the ability of STAT-3 inhibition to treat fibrosis (29). Inhibition of IL-6 *trans*-signaling (18) and other cytokines upstream of STAT-3 reduces lung fibrosis in the ITB model (30, 31). However, these cytokines do not only signal through STAT-3 but also activate other cellular pathways, such as MAPK/ERK and PI3K/Akt (32). Several nonspecific inhibitors, such as alkaloids (matrine), nonsteroidal anti-inflammatory drugs (sulindac), and inorganic compounds ($As_2O_3$) have been shown to decrease lung fibrosis accompanied by a decrease in STAT-3 (33–35), but these molecules also inhibit multiple signaling pathways. Although these studies suggest that STAT-3 is a therapeutic target in lung fibrosis, they do not clearly demonstrate that specific targeting of STAT-3 is effective in diminishing lung fibrosis.

C-188-9 is a synthetic small molecule inhibitor of STAT-3 phosphorylation and activation by targeting the phospho-Tyr peptide binding pocket of the Src homology 2 domain of STAT-3 (36). C-188-9 had been shown to inhibit STAT-3 activation in acute myeloid leukemia cells and in *in vivo* models of breast cancer and cachexia associated with chronic kidney disease (36–39). In the current manuscript, C-188-9 inhibited STAT-3 activation and decreased the development of pulmonary fibrosis in bleomycin (BLM)-exposed mice. Furthermore, *in vitro* studies demonstrated an important role for STAT-3 in type II AEC injury and fibroblast activation and differentiation. These data suggest that STAT-3 may be a potential therapeutic target in pulmonary fibrosis.

## MATERIALS AND METHODS

### Mice

Wild-type C57BL/6 mice were purchased from Jackson ImmunoResearch Laboratories (West Grove, PA, USA). Animal care was in accordance with institutional and U.S. National Institutes of Health (Bethesda, MD, USA) guidelines and approved by the Baylor College of Medicine Animal Welfare Committee. Mice were housed in ventilated cages equipped with microisolator lids and maintained under strict containment protocols.

### Intraperitoneal BLM lung fibrosis model

Wild-type C57BL/6 male mice (age 5 wk) were injected with 0.035 U/g BLM or PBS (control) *via* the intraperitoneal route twice per week for 4 wk (40). Arterial oxygen saturation was obtained using MouseOx (Starr Life Sciences Corp., Oakmont, PA, USA). On d 30, mice were anesthetized with Avertin, and lungs were lavaged 4 times with 0.3 ml PBS [0.95–1 ml bronchoalveolar lavage (BAL) fluid was recovered]. BAL total cell counts were determined using a hemocytometer. Cytospins of BAL were prepared and stained with Diff-Quick (Dade Behring, Deerfield, IL, USA) for cellular differential counts. After lavage, the lungs were infused with 10% buffered formalin at 25 cm $H_2O$ pressure, fixed overnight at 4°C, and embedded in paraffin. There were 5 μm sections obtained for histology, including hematoxylin and eosin (H&E; Shandon Lipshaw, Pittsburgh, PA, USA) and Masson's trichrome (Electron Microscopy Sciences, Hatfield, PA, USA). H&E-stained lung sections were used to determine the Ashcroft score using 20 microscope fields per section in a blinded manner (41, 42). The Sircol Collagen Assay (Biocolor Life Science Assays, County Antrim, United Kingdom) was used to measure soluble collagen in BAL fluid. Total RNA was isolated from frozen mouse lung tissue utilizing Trizol (Invitrogen, Life Technologies, Carlsbad, CA, USA) and used for quantitative real-time PCR analysis using TaqMan primers (Applied Biosystems, Foster City, CA, USA).

### C-188-9 (STAT-3 inhibitor) treatment

C57BL/6J mice exposed to BLM or PBS control as described above were treated with daily intraperitoneal injections of 1.25 mg C-188-9 starting on d 15 until d 29. Vehicle (DMSO) was used as a treatment control. Experiments were performed 4 times, with 5 mice per experimental group each time (PBS/vehicle, PBS/C-188-9, BLM/DMSO, and BLM/C-188-9).

### Human lung tissue

Surgical biopsy specimens from IPF lung tissue samples were obtained from the U.S. National Institutes of Health National Heart, Lung, and Blood Institute and processed as described (20). Patients with IPF were diagnosed and classified using high-resolution computed tomography scans, pathologic examination, and spirometry analysis: FEV1 (forced expiratory volume in 1 s) and FVC (forced vital capacity). Mild IPF is defined as FEV1 and FVC percentage (%) predicted >80. Severe IPF is defined as FEV1 and FVC percentage (%) predicted <50 (20). Normal lung tissue from healthy donor lungs at the time of organ transplantation was obtained from LifeGift (Houston, TX, USA) through the International Institute for the Advancement of Medicine (Edison, NJ, USA). Use of human tissues was approved by the institutional review boards at The University of Texas Health Science Center, Houston, and Baylor College of Medicine.

### Immunohistochemistry

Tissue sections (5 μm) were rehydrated, and endogenous peroxidases were quenched with 3% hydrogen peroxide. Antigen retrieval was performed (Dako, Carpinteria, CA, USA), and endogenous avidin and biotin were blocked with the

(*continued from previous page*)

HIF-1α, hypoxia-inducible factor-1α; HSP-70, heat shock protein-70; IHC, immunohistochemistry; ILD, interstitial lung disease; IPF, idiopathic pulmonary fibrosis; ITB, intratracheal bleomycin; MLE-12, murine lung epithelial-12; PAI-1, plasminogen activator inhibitor-1; phospho-STAT-3, phosphorylated STAT-3; shRNA, short hairpin RNA; SPC, surfactant protein C

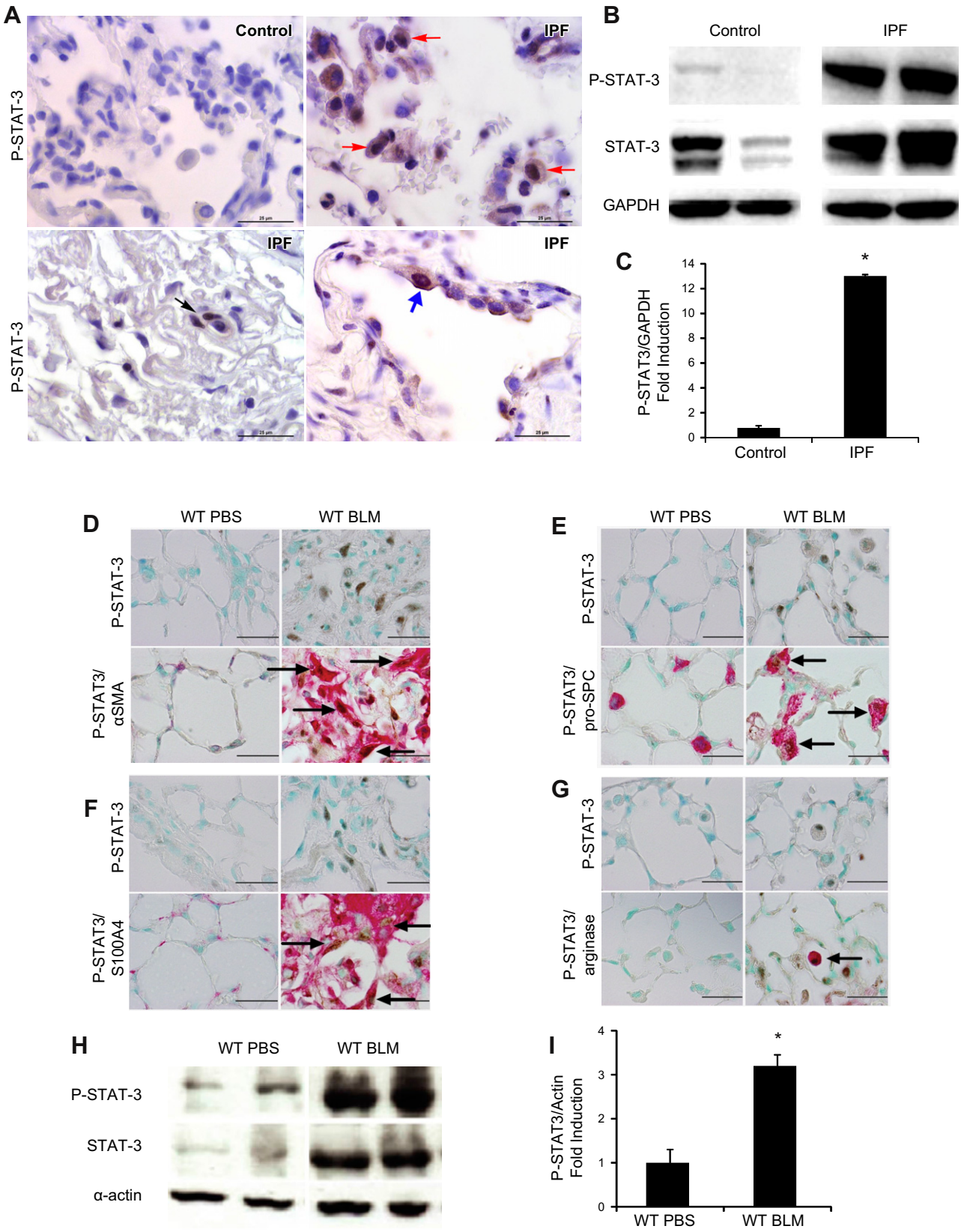


**Figure 1.** Characterization of STAT-3 activation in human patients with IPF and the BLM model. *A*) Immunolocalization of phospho-STAT-3 (P-STAT-3) expression on alveolar fibroblasts (black arrows), alveolar macrophages (red arrows), and AECs (blue arrows) in lung sections from healthy control and patients with severe IPF. Images are representative of 4 patients from each group. *B*) Western blot analysis of phospho-STAT-3 expression in human patients with mild and severe IPF. STAT-3 and GAPDH were used as controls ($n \geq 4$). *$P \leq 0.05$ control *vs.* IPF. *C*) Phospho-STAT-3 band intensity was quantified using ImageJ analysis. Values are

(*continued on next page*)

Biotin-Blocking System (Dako). Slides were then incubated overnight at 4°C with primary antibodies for phospho-STAT-3, type I collagen (1:100 dilution; Abcam Inc., Cambridge, MA, USA), or α–smooth muscle actin (α-SMA; 1:1000 dilution; Sigma-Aldrich, St. Louis, MO, USA). All sections were incubated with ABC Elite Streptavidin reagents (Vector Laboratories, Burlingame, CA, USA) and appropriate secondary antibodies. Sections were developed with 3,3′-diaminobenzidine (Sigma-Aldrich) and counterstained with methyl green or hematoxylin. For α-SMA staining, slides were processed with the Mouse on Mouse Kit and the Vector Red Alkaline Phosphatase Substrate Kit (Vector Laboratories).

For coimmunolocalization, slides were incubated overnight at 4°C with primary antibodies for phospho–STAT-3 or isotype (1:100 dilution; Abcam Inc.) using the ImmPress HRP rabbit detection kit and developed with the ImmPact DAB substrate kit (both from Vector Laboratories). Subsequently, the second primary antibodies were incubated (4°C overnight) against F4/80, SPC, FSP-1, or isotype (1:100 dilution; Abcam Inc.) using the ImmPRESS AP rabbit detection kit and developed using the ImmPact Vector Red substrate kit (both from Vector Laboratories). For α-SMA staining (1:1000 dilution; Sigma-Aldrich) on human tissue, the ImmPress AP mouse detection kit (Vector Laboratories) was used and developed using the ImmPact Vector Red substrate kit. Isotype controls include rabbit IgG for all antibodies and mouse IgG for α-SMA.

### Western blot analysis

Cells were lysed with 1× RIPA Lysis Buffer (EMD Millipore, Billerica, MA, USA) freshly supplemented with 1× protease and 1× phosphatase inhibitor mixture (Roche Diagnostics, Basel, Switzerland). A 50 μg lysate of total protein was electrophoresed on 10% SDS-PAGEs and transferred to PVDF membrane. For primary antibody incubation (overnight at 4°C), rabbit pAbs were used against phospho-STAT-3 (1:500; Abcam Inc.), STAT-3 (1:500; Abcam Inc.), and IL-6 (1:500; Abcam Inc.), whereas a mouse monoclonal anti-human was used against α-actin (1:5000; Sigma-Aldrich) and anti-mouse against glyceraldehyde 3-phosphate dehydrogenase (GAPDH; 1:1000; Abcam Inc.). Species-specific horseradish peroxidase-conjugated secondary antibodies (Jackson ImmunoResearch Laboratories) were applied for 1 h at room temperature, and blots were developed using ECL Western blotting substrate (Thermo Fisher Scientific, Waltham, MA, USA). ImageJ analysis (U.S. National Institutes of Health) was used to quantify Western blots.

### Cell culture

A549, a human AEC line, and MLE-12 (murine lung epithelial-12), an immortalized murine AEC line, were obtained from American Type Culture Collection (Manassas, VA, USA). Primary type II AECs and lung fibroblasts were isolated from C57BL/6 mice as previously described (43, 44). Cells were cultured at 37°C with 5% $CO_2$ in DMEM containing 10% fetal bovine serum and 1% penicillin/streptomycin. Stable knockdown cell lines were created in A549 cells with pLK0.1-based lentiviral particles containing short hairpin RNAs (shRNAs) targeting STAT-3 (#TRCN0000329888) or Mission TRC2 Transduction Particle containing control shRNA (#SHC216V; both from Sigma-Aldrich). These cells were cultured in F12 medium (American Type Culture Collection) containing 10% fetal bovine serum, 1% penicillin/streptomycin, and 0.1% Fungizone. For experiments, cells were stimulated with medium alone, IL-6 (20 μg/ml) and sIL-6Rα (20 μg/ml), or TGF-β (10 ng/ml) (all from R&D Systems, Minneapolis, MN, USA) with and without the addition of C-188-9 (20 μM), SMAD2 inhibitor (616464, 10 μM; EMD Millipore), and SMAD3 inhibitor (566405, 10 μM; EMD Millipore). Cells were harvested at 24 h post treatment for RNA analysis and for Western blotting. All *in vitro* experiments were performed in 4 individual experiments.

### Statistics

Values are expressed as means ± SEM. As appropriate, groups were compared by ANOVA; follow-up comparisons between groups were conducted using 2-tailed Student's *t* test. A value of $P \leq 0.05$ was considered to be significant.

## RESULTS

### Increased STAT-3 activation in the fibrotic lungs of patients with IPF and the BLM mouse model

To determine if activated STAT-3 is expressed in the fibrotic lungs of patients with IPF, lung sections were stained with anti–phospho-STAT-3 antibody (**Fig. 1*A***). Staining with isotype control antibody demonstrated minimal background staining (Supplemental Fig. 1). Furthermore, expression of phospho-STAT-3 was not observed in nonfibrotic healthy control lungs. In contrast, nuclear phospho-STAT-3 expression was observed in fibrotic lungs, localizing to alveolar macrophages and fibroblasts. In addition, phospho-STAT-3 expression localized to the nuclei of hyperplastic AECs adjacent to fibrotic foci in the lungs of patients with IPF. Western blot analysis of lysates of lung biopsies obtained from affected areas of patients with severe IPF demonstrated increased phospho-STAT-3 expression relative to lung biopsies from healthy control subjects (Fig. 1*B*, *C*). These results demonstrate that phospho-STAT-3 is elevated in the fibrotic lungs of patients with IPF.

To determine if STAT-3 is activated during the development of lung fibrosis in mice, phospho-STAT-3 immunohistochemistry (IHC) and coimmunolocalization studies for α-SMA, S100A4, pro-SPC, and arginase were performed on fibrotic lungs from mice in the intraperitoneal BLM model. Similar to IPF lungs, murine fibrotic lungs had increased nuclear phospho-STAT-3 in myofibroblasts (α-SMA, Fig. 1*D*), AECs (pro-SPC, Fig. 1*E*), fibroblasts (S100A4, Fig. 1*F*), and alveolar macrophages (arginase, Fig. 1*G*). Levels of STAT-3 and phospho-STAT-3 were increased in lung lysates of wild-type mice

presented as the percentages of GAPDH ± SEM ($n \geq 4$). *$P \leq 0.05$ control *vs.* IPF. Coimmunolocalization expression of phospho-STAT-3 and α-SMA (*D*), pro-SPC (*E*), S100A4 (*F*), and arginase (*G*) in lung sections from wild-type mice treated with PBS and BLM. Images are representative of 8 mice from each group. Scale bars, 50 μm. *H*) Western blot analysis using an antibody against phospho-STAT-3 in whole-lung lysates. STAT-3 and α-actin were used as controls. *I*) Phospho-STAT-3 band intensity was quantified using ImageJ analysis. Values are presented as the percentages of α-actin ± SEM ($n \geq 4$). *$P \leq 0.05$ PBS *vs.* BLM. Arrows in *D*–*G* identify the phospho-STAT3-positive cells.

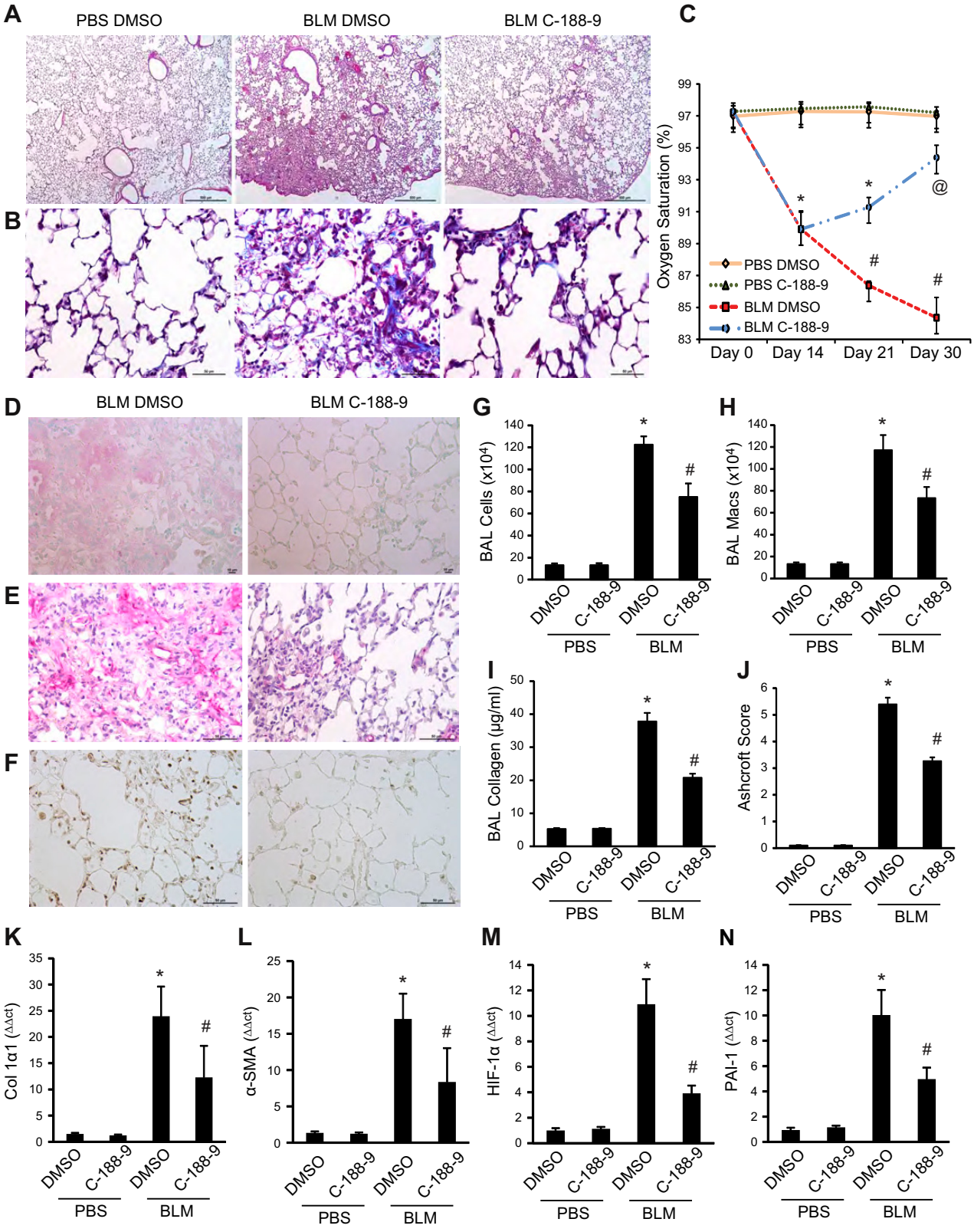


**Figure 2.** Pulmonary phenotype following intraperitoneal BLM exposure in mice treated with STAT-3 inhibitor. This figure displays representative histology of lungs from mice treated with PBS and vehicle (DMSO) or C-188-9 (left) and from BLM-exposed mice treated with DMSO (middle) or STAT-3 inhibitor, C-188-9 (right). Examination of lung histology through H&E staining (*A*) and Masson's trichrome (*B*) for Col1α1 (*D*), α-SMA (*E*), and phospho-STAT-3 (*F*). These images revealed that inhibition of STAT-3 displayed a reduction in pulmonary injury and fibrosis. Images are representative of 8 mice from each group. Scale bars, 500 µm (magnification, ×5) (*A*) and 50 µm (magnification, ×40) (*B* and *D*–*F*). *C*) Pulse oxygen measurements at different time points

(*continued on next page*)

exposed to BLM compared to PBS (Fig. 1*H, I*). Finally, similar to the murine lungs, coimmunolocalization studies in IPF lungs also demonstrated phospho-STAT-3 staining in IPF lungs on alveolar macrophages, AECs, and myofibroblasts (Supplemental Fig. 1). Together, these data demonstrate that activated STAT-3 is increased in the fibrotic human and murine lungs.

### Treatment with C-188-9, a STAT-3 inhibitor, attenuates pulmonary fibrosis

To determine the extent to which inhibition of STAT-3 activation attenuates pulmonary fibrosis, C-188-9 was administered to wild-type mice in the intraperitoneal BLM model from d 15 to 30. Treatment with C-188-9 decreased all fibrotic endpoints assessed in the model (**Fig. 2**). Representative histologic images are shown in Fig. 2*A* and quantified using Ashcroft scoring in Fig. 2*J*. Wild-type mice exposed to BLM displayed characteristic increases in ECM deposition, as visualized on Masson's trichrome staining (Fig. 2*B*), and increased type I collagen immunoreactivity (Fig. 2*D*), both of which were decreased in mice treated with C-188-9. α-SMA immunoreactivity, consistent with the presence of myofibroblasts, was increased by BLM and decreased in mice treated with C-188-9 (Fig. 2*E*). Finally, IHC with anti–phospho-STAT-3 antibody confirmed that treatment with C-188-9 inhibited STAT-3 activation *in vivo* (Fig. 2*F*).

Additional quantifiable fibrosis endpoints assessed are shown in Fig. 2. Mice injected with BLM had reduced arterial oxygen saturation that upon treatment with C-188-9 was restored to near unexposed levels (Fig. 2*C*). C-188-9 treatment decreased BAL total cell counts induced by BLM (Fig. 2*G*), primarily through a reduction in macrophage numbers (Fig. 2*H*). C-188-9 treatment reduced soluble collagen in the BAL (Fig. 2*I*) and *Col1α1* (collagen 1α1) mRNA in the lung tissue (Fig. 2*K*) of mice exposed to BLM. Finally, whole-lung total RNA analysis revealed that BLM-exposed mice treated with C-188-9 exhibited significant reduction in other markers of fibrosis, including α-SMA (Fig. 2*L*), *Twist* (Supplemental Fig. 2*A*), *Snail* (Supplemental Fig. 2*B*), as well as markers of AEC injury such as HIF-1α (hypoxia-inducible factor 1α) (45), PAI-1 (plasminogen activator inhibitor-1) (46) (Fig. 2*M, N*, respectively), and HSP-70 (heat shock protein 70) (47) (Supplemental Fig. 2*C*). Together, these data clearly demonstrate that inhibition of STAT-3 effectively attenuates the development of fibrosis in the intraperitoneal BLM model of lung fibrosis.

### Inhibition of STAT-3 decreases type II AEC injury

Given the importance of the type II AECs in the development of pulmonary fibrosis (9–15) and the expression of phospho-STAT-3 in AECs in fibrotic lungs, the role of STAT-3 regulating type II AECs was investigated. Stimulation of the immortalized murine type II AEC line, MLE-12, with TGF-β or the combination of IL-6 and the soluble IL-6Rα induced the expression of injury markers such as *HIF-1α* and *PAI-1* (**Fig. 3*C, D***, respectively) and fibrotic genes, including *Col 1α1* (Fig. 3*A*), *Twist* (Fig. 3*B*), *α-SMA* (Supplemental Fig. 3*A*), and *Snail* (Supplemental Fig. 3*B*). As expected, inhibition of STAT-3 activation with C-188-9 blocked the increase in *HIF-1α*, *PAI-1*, *Col 1α1*, *α-SMA*, *Twist*, and *Snail* mRNA induced by IL-6/sIL-6Rα complex. Interestingly, C-188-9 also blocked the increase in *HIF-1α*, *PAI-1*, *Col 1α1*, *α-SMA*, *Twist*, and *Snail* mRNA induced by TGF-β (Fig. 3*A–D* and Supplemental Fig. 3*A–C*). In addition, C-188-9 was also able to block the increase in *HIF-1α*, *PAI-1*, *Col 1α1*, *α-SMA*, *Twist*, and *Snail* mRNA induced by IL-6/sIL-6Rα complex or TGF-β in primary murine type II AECs *in vitro* (Fig. 3*E–H* and Supplemental Fig. 3*D–F*). These data demonstrate that STAT-3 inhibition with C-188-9 decreases type II AEC injury and mesenchymal gene expression *in vitro*.

The ability of STAT-3 inhibition with C-188-9 to block TGF-β stimulation of type II AECs was unexpected. To confirm that STAT-3 inhibition, and not an off-target effect of C-188-9, blocks TGF-β stimulation in type II AECs, STAT-3 mRNA silencing using shRNA was employed. Stimulation of A549 cells, a lung epithelial cancer cell line with features of type II AECs, with IL-6/sIL-6Rα complex or TGF-β increased expression *Col 1α1*, *Twist*, *HIF-1α*, and *PAI-1* mRNA (Fig. 3*I–L*). Inhibition of STAT-3 expression using shRNA attenuated the increase in *Col 1α1*, *Twist*, *HIF-1α*, and *PAI-1* mRNA induced by IL-6/sIL-6Rα complex or TGF-β. Finally, shSTAT3 A549 cells exhibited reduced IL-6/sIL-6Rα complex or TGF-β–induced expression of *α-SMA*, *Snail*, and *HSP-70* mRNA (Supplemental Fig. 3*G–I*). These data confirm that STAT-3 activation plays an important role in the expression of injury and fibrotic markers induced by IL-6 activation and also TGF-β activation in type II AECs.

### Inhibition of STAT-3 activation decreases myofibroblast differentiation

Given the importance of fibroblast and myofibroblast differentiation in the development of lung fibrosis, we next sought to determine the extent to which STAT-3

(d 0, 14, 21, and 30). Data are presented as the percentages of oxygen saturation ± SEM ($n \geq 8$). *$P \leq 0.05$ PBS DMSO or C-188-9 *vs.* BLM DMSO or C-188-9; $^{\#}P \leq 0.05$ BLM DMSO *vs.* BLM C-188-9 and PBS DMSO or C-188-9; $^{@}P \leq 0.05$ BLM C-188-9 *vs.* BLM DMSO and PBS DMSO or C-188-9. *G*) Total cell numbers obtained from BAL and macrophages (Macs; *H*). *I*) Soluble collagen protein levels were measured using Sircol Assay. Data are presented as mean milligrams of collagen per milliliters of BAL fluid ± SEM. *$P \leq 0.05$ PBS DMSO *vs.* BLM DMSO; $^{\#}P \leq 0.05$ BLM DMSO *vs.* BLM C-188-9 ($n \geq 8$). *J*) Ashcroft scores were used to determine the degree of fibrosis. Data are presented as means ± SEM. *$P \leq 0.05$ PBS DMSO *vs.* BLM DMSO; $^{\#}P \leq 0.05$ BLM DMSO *vs.* BLM C-188-9 ($n \geq 8$). Total RNA was isolated from whole-lung mice, and transcripts were determined for *Col1α1* (*K*), *α-SMA* (*L*), *HIF-1α* (*M*), and *PAI-1* (*N*). Transcripts were measured in parallel with 18S rRNA, and values are presented as means of fold change transcripts ± SEM ($n \geq 8$). *$P \leq 0.05$ PBS DMSO *vs.* BLM DMSO; $^{\#}P \leq 0.05$ BLM DMSO *vs.* BLM C-188-9.

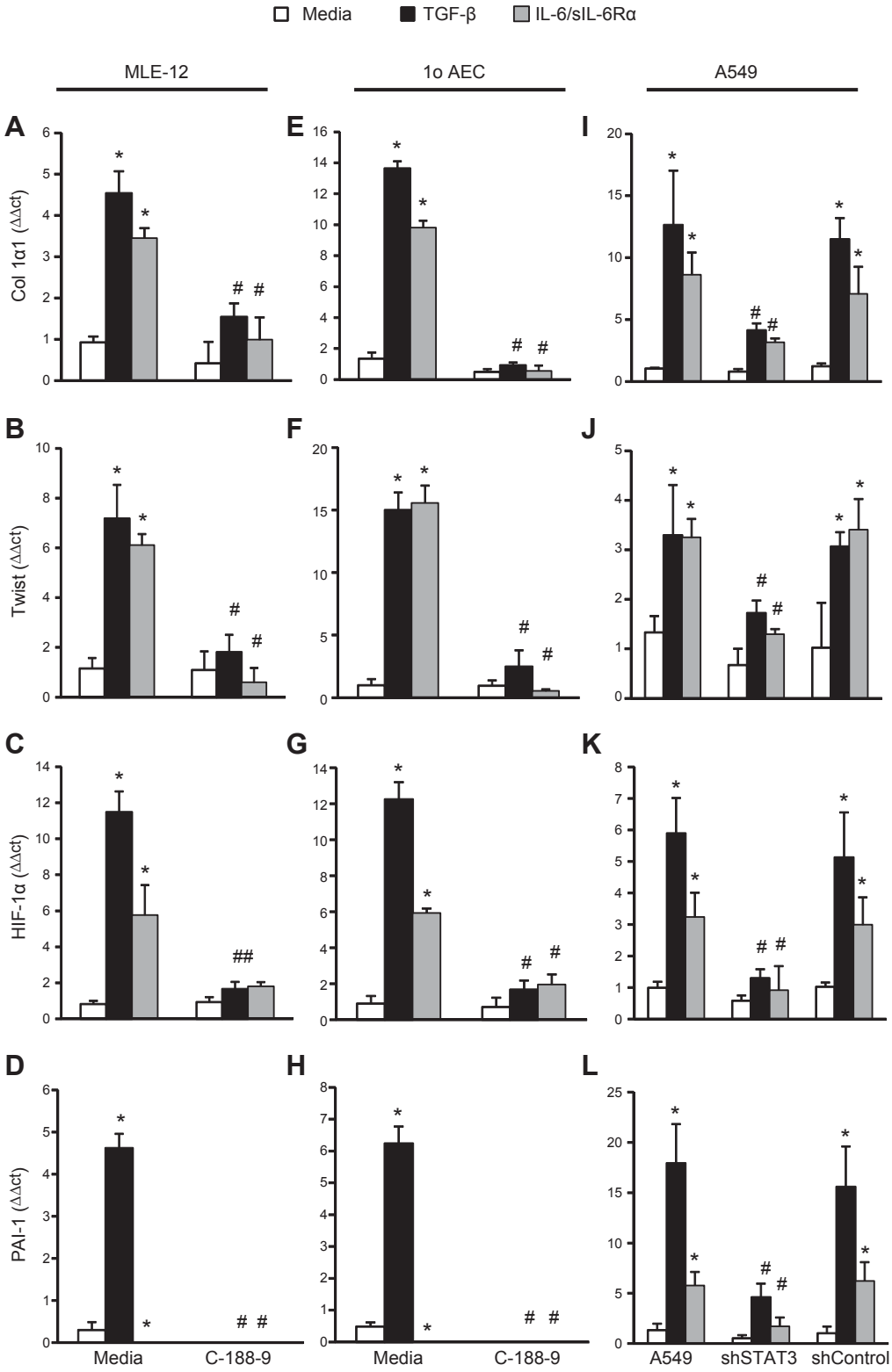


**Figure 3.** Profibrotic mediators on different cells following STAT-3 inhibition or knockdown. MLE-12 was plated and subsequently stimulated with TGF-β (10 ng/ml), IL-6/sIL-6Rα complex (40 μg/ml), and C-188-9 inhibitor (20 μM); 24 h later, RNA was isolated, and transcripts were determined for *Col1α1* (*A*), *Twist* (*B*), *HIF-1α* (*C*), and *PAI-1* (*D*). Similarly, primary AECs were isolated from mice. After isolation, AECs were treated similarly as above; 24 h later, RNA was isolated, and transcripts were determined for *Col1α1* (*E*), *Twist* (*F*), *HIF-1α* (*G*), and *PAI-1* (*H*). A549 shSTAT-3 and shControl were plated and subsequently stimulated with TGF-β (10 ng/ml) or IL-6/sIL-6Rα complex (40 μg/ml); 24 h later, RNA was isolated, and transcripts were determined for *Col1α1* (*I*), *Twist* (*J*), *HIF-1α* (*K*), and *PAI-1* (*L*). Transcripts were measured in parallel with 18S rRNA, and values are presented as means of fold change transcripts ± SEM ($n \geq 4$). *$P \leq 0.05$ medium *vs.* TGF-β, IL-6/sIL-6Rα; #$P \leq 0.05$ TGF-β *vs.* TGF-β C-188-9, shSTAT3; and IL-6/sIL-6Rα *vs.* IL-6/sIL-6Rα C-188-9, shSTAT3.

regulates fibroblast-to-myofibroblast differentiation. To induce myofibroblast differentiation, primary murine lung fibroblasts were treated with TGF-β or the IL-6/sIL-6Rα complex. Both stimuli increased myofibroblast differentiation markers (**Fig. 4**, *Col1α1*, *α-SMA*, *Twist*, and *Snail*). Treatment of lung fibroblast cultures with C-188-9 attenuated these transcripts induced by TGF-β and IL-6 *trans*-signaling (Fig. 4). No effects were seen in *FSP-1* (Supplemental Fig. 3*J*), which is a fibroblast marker serving as a control. Thus, these results indicate that STAT-3 regulates both IL-6–mediated and TGF-β–mediated myofibroblast differentiation in murine lung fibroblasts.

### STAT-3 and SMAD3 inhibition leads to diminished TGF-β–induced STAT-3 activation

To further characterize the pathways that are used by TGF-β to activate STAT-3, Western blotting was performed on lung fibroblasts stimulated with TGF-β or IL-6/sIL-6Rα complex (**Fig. 5**). As expected, IL-6 *trans*-signaling increased STAT-3 phosphorylation at Tyr705. Consistent with the hypothesis that TGF-β induces phosphorylation of STAT-3, increased phospho-STAT-3 was observed in lysates of lung fibroblasts stimulated with TGF-β. To characterize the signaling pathways that contribute to the activation of STAT-3, lung fibroblasts were stimulated in the presence of STAT-3 inhibitor C-188-9 or SMAD2 and SMAD3 inhibitors. As expected, IL-6 activation of STAT-3 was blocked by the STAT-3 inhibitor C-188-9, but not SMAD2 or SMAD3 inhibitors. In contrast, the TGF-β–induced STAT-3 activation was blocked by C-188-9 as well as the SMAD2 and SMAD3 inhibitors. These data suggest that the TGF-β receptor complex in lung fibroblasts activates STAT-3 in an SMAD-dependent process.

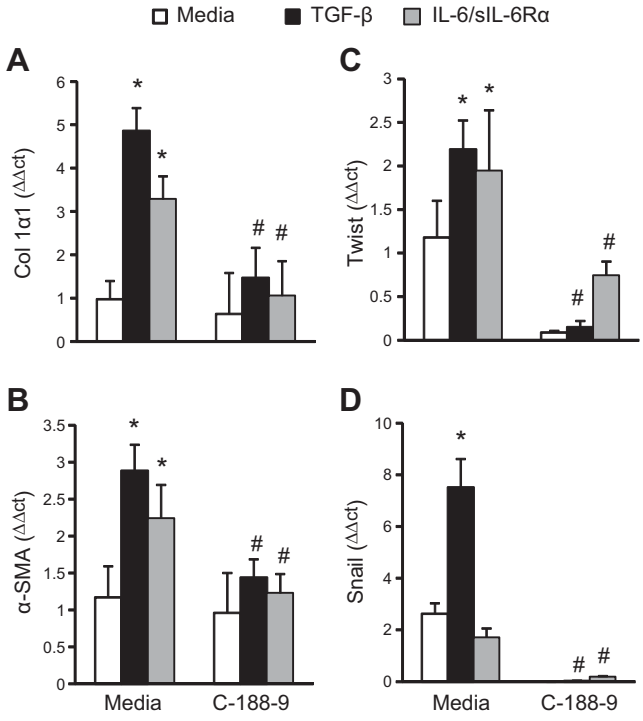


**Figure 4.** Myofibroblast differentiation on lung fibroblasts following STAT-3 inhibition. Primary lung fibroblasts were isolated, plated, and subsequently stimulated with TGF-β (10 ng/ml), IL-6/sIL-6Rα complex (40 μg/ml), and C-188-9 inhibitor (20 μM); 24 h later, RNA was isolated, and transcripts were determined for *Col1α1* (*A*), *α-SMA* (*B*), *Twist* (*C*), and *Snail* (*D*). Transcripts were measured in parallel with 18S rRNA, and values are presented as means of fold change transcripts ± SEM ($n \geq 4$). *$P \leq 0.05$ medium *vs.* TGF-β, IL-6/sIL-6Rα; #$P \leq 0.05$ TGF-β *vs.* TGF-β C-188-9; and IL-6/sIL-6Rα *vs.* IL-6/sIL-6Rα C-188-9.

## DISCUSSION

In the current manuscript, we demonstrate that STAT-3 is activated in fibrotic lung tissue and that STAT-3 phosphorylation plays an important role in the development of pulmonary fibrosis. Furthermore, *in vitro* data demonstrate that TGF-β–induced activation of STAT-3 contributes to the expression of injury-related and mesenchymal genes in AECs as well as the differentiation lung fibroblasts into myofibroblasts. These data not only have important implications for our understanding of STAT-3 signaling in the development of pulmonary fibrosis but also for the potential of C-188-9, a STAT-3 small molecule inhibitor, as a therapeutic in pulmonary fibrosis.

STAT-3 is a latent cytoplasmic transcription factor that is activated by multiple cytokines, including the IL-6 family of cytokines. The IL-6 family of cytokines includes IL-6, IL-11, Oncostatin M, leukemia inhibitory factor, IL-27, and IL-31, among others (48–50). Activation of STAT-3 regulates multiple biologic functions, including cell survival, migration, proliferation, and differentiation (51). IL-6 also has been shown to be a profibrotic cytokine inducing fibroblast proliferation and myofibroblast differentiation (27, 52). It has been shown that IL-6, *via* IL-6 *trans*-signaling, contributes to the development of fibrosis (17, 18). However, other IL-6 family members also contribute to the development of fibrosis. For instance, Oncostatin M is elevated in fibrotic tissues and induces pulmonary inflammation and fibrosis (53), and IL-11 is released from fibroblasts, and its overexpression induces collagen deposition in mice (54). Therefore, targeting common downstream mediators of the IL-6 family of cytokines, such as STAT-3, rather than individual cytokines may be more appealing.

C-188-9 is a synthetic small molecule STAT-3 inhibitor that targets the phospho-Tyr peptide binding pocket within the STAT-3 Src homology 2 domain (36, 55) and inhibits STAT-3 activation-receptor recruitment and homodimerization (37). C-188-9 has been used to block STAT-3 in acute myeloid leukemia cells and muscle wasting associated with chronic kidney disease (38, 39). In the current manuscript, C-188-9 decreased biochemical and molecular markers of fibrosis in the intraperitoneal BLM model. The intraperitoneal model is associated with progressive subpleural pulmonary fibrosis, which resembles human pulmonary fibrosis to a greater extent than the intratracheal (40, 56, 57). The administration of C-188-9 was after the onset

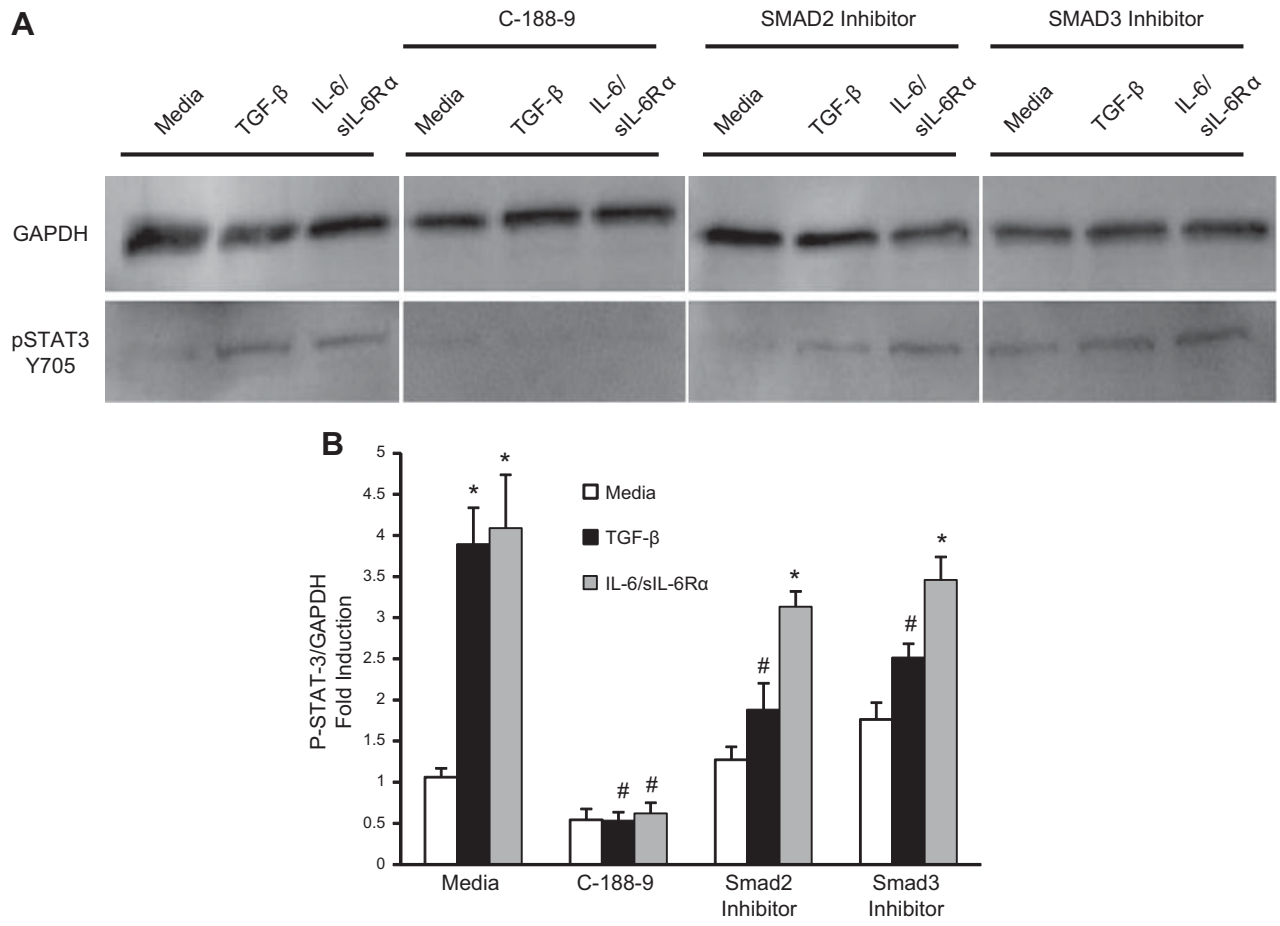


**Figure 5.** STAT-3 inhibition on lung fibroblasts. *A*) Lung fibroblasts were plated, treated for 1 h with different inhibitors (C-188-9, 20 μM; SMAD2 and 3 inhibitor, 10 μM), and subsequently stimulated with TGF-β (10 ng/ml) and IL-6/sIL-6Rα complex (40 μg/ml); 24 h later, STAT-3 activation was measured in protein lysates using Western blot analysis with a phospho-STAT-3 (pSTAT-3) antibody (Tyr705) on lung fibroblasts. GAPDH levels were used as a loading control. *B*) Phospho-STAT-3 (P-STAT-3; Tyr705) band intensity was quantified using ImageJ analysis on lung fibroblasts treated with different inhibitors. Values are presented as the percentages of GAPDH ± SEM ($n \geq 4$). $^{*}P \leq 0.05$ medium *vs.* TGF-β, IL-6/sIL-6Rα; $^{\#}P \leq 0.05$ TGF-β *vs.* TGF-β C-188-9, SMAD2 and 3 inhibitor; and IL-6/sIL-6Rα *vs.* IL-6/sIL-6Rα C-188-9.

of fibrosis to model treatment of pulmonary fibrosis rather than prevention. Impressively, we observed that the clinical endpoint of hypoxia was markedly improved in mice after the initiation of C-188-9 treatment. These data combined with the other quantitative endpoints of fibrosis strongly suggest that C-188-9 and/or targeting STAT-3 is a potential therapeutic strategy in patients with pulmonary fibrosis.

In the current manuscript, activated (phosphorylated) STAT-3 was shown to be elevated in lung biopsies from patients with severe IPF and fibrotic murine lungs in the intraperitoneal BLM model. These data are consistent with prior reports that demonstrated elevated phospho-STAT-3 in patients with IPF and also the adenosine deaminase-deficient mouse model (17, 18, 28). Dual-labeling IHC of murine fibrotic lungs demonstrated that STAT-3 was activated on type II AECs, fibroblasts, myofibroblasts, and alveolar macrophages in fibrotic lungs. Furthermore, C-188-9 decreased STAT-3 activation in alveolar macrophages, lung fibroblasts, and type II AECs. These data point to a role of STAT-3 activation in these cell populations and their respective contributions in fibrosis pathogenesis. Current literature suggests that injury to type II AECs leads to the expression of injury markers, including HIF-1α, PAI-1, and HSP-70 (45–47, 58–60), and fibrotic markers, including Col1α1, α-SMA, TWIST, and SNAIL (4, 12, 14, 61). Within this milieu, fibroblasts and myofibroblasts accumulate, to form the fibroblastic foci, deposit ECM, and disrupt the alveolar architecture. The *in vitro* studies reported herein demonstrate that STAT-3 is involved in both TGF-β– and IL-6 *trans*-signaling–induced expression of these injury and fibrotic markers in AECs and lung fibroblasts. These *in vitro* data are consistent with this model and further support a novel role for STAT-3 in regulating the expression of injury and fibrotic genes in AECs and fibroblasts stimulated with TGF-β.

The ability of TGF-β to activate STAT-3 was validated in multiple cell lines (AECs and fibroblasts) and using multiple techniques. Western blotting of murine lung fibroblasts demonstrated that TGF-β stimulation increases STAT-3 phosphorylation at Tyr705, and this was dependent on SMAD2 and SMAD3. The crosstalk between

TGF-β and STAT-3 (or IL-6) pathways has been previously suggested, though the mechanisms that underlie this crosstalk are not known. A recent study demonstrated that TGF-β required STAT-3 activation to induce connective tissue growth factor expression during the development of liver fibrosis (62). Alternatively, TGF-β has been shown to inhibit IL-6 *trans*-signaling (63) and that STAT-3 attenuates TGF-β activity in gastric adenomas (64). A physical interaction of STAT-3 with the TGF-β receptor I chain has been suggested in 293T cells, whereas in Hep3B cells, an interaction between STAT-3 and SMAD3 has been suggested (*via* p300) (65). These results were primarily obtained in cells overexpressing STAT-3 and varied depending on the cell type studied. Alternatively, it is also possible that TGF-β indirectly leads to the activation of STAT-3 by inducing IL-6 or IL-6 family members (66, 67). The extent to which STAT-3 and proteins in the TGF-β pathway interact in AECs or lung fibroblasts is not well understood and is currently being investigated. However, collectively, these reports and the current data demonstrate the potential for reciprocal interactions between STAT-3/IL-6 and SMAD/TGF-β pathways and stress the need for continued investigation.

In conclusion, our findings support a role for STAT-3 signaling in regulating type II AECs and fibroblasts during the development of pulmonary fibrosis. We hypothesize that STAT-3 activation occurs upon injury to the type II AECs, promoting the profibrotic milieu that leads to accumulation of fibroblasts and myofibroblasts. STAT-3 is also active in lung fibroblasts and likely contributes to the fibrotic process through myofibroblast differentiation from fibroblasts. These findings highlight the importance of not only IL-6 and TGF-β but also STAT-3 as an important mediator of pulmonary fibrosis. The current data add to our understanding of the lung fibrosis pathogenesis and suggest that STAT-3 inhibition through small molecule inhibitors such as C-188-9 may be a therapeutic strategy for fibrotic diseases such as IPF. FJ

This work was supported by the U.S. Department of Defense, Peer Reviewed Medical Research Program Grant W81XWH-12-1-0516 (to M.P. and S.K.A.), and U.S. National Institutes of Health Grants R01AR062056 (to S.K.A., S.T., and A.T.G.), K08AR054404 (to S.K.A.), and 2T32AI053831-11A1 (to M.P.).

## REFERENCES

1. Panos, R. J., Mortenson, R. L., Niccoli, S. A., and King, Jr., T. E. (1990) Clinical deterioration in patients with idiopathic pulmonary fibrosis: causes and assessment. *Am. J. Med.* **88**, 396–404
2. Lynch, J., and Toews, G. (1998) Idiopathic pulmonary fibrosis. In *Pulmonary Diseases and Disorders*, Vol. 1 (Fishman, A. P., Elias, J. A., Fishman, J. A., Grippi, M. A., Kaiser, L. R., and Senior, R. M., eds.), pp. 1069–1084, McGraw-Hill, New York
3. Fernández Pérez, E. R., Daniels, C. E., Schroeder, D. R., St Sauver, J., Hartman, T. E., Bartholmai, B. J., Yi, E. S., and Ryu, J. H. (2010) Incidence, prevalence, and clinical course of idiopathic pulmonary fibrosis: a population-based study. *Chest* **137**, 129–137
4. Lee, A. S., Mira-Avendano, I., Ryu, J. H., and Daniels, C. E. (2014) The burden of idiopathic pulmonary fibrosis: an unmet public health need. *Respir. Med.* **108**, 955–967
5. Coultas, D. B., Zumwalt, R. E., Black, W. C., and Sobonya, R. E. (1994) The epidemiology of interstitial lung diseases. *Am. J. Respir. Crit. Care Med.* **150**, 967–972
6. Olson, A. L., Swigris, J. J., Lezotte, D. C., Norris, J. M., Wilson, C. G., and Brown, K. K. (2007) Mortality from pulmonary fibrosis increased in the United States from 1992 to 2003. *Am. J. Respir. Crit. Care Med.* **176**, 277–284
7. Sheppard, D. (2001) Pulmonary fibrosis: a cellular overreaction or a failure of communication? *J. Clin. Invest.* **107**, 1501–1502
8. Horowitz, J. C., and Thannickal, V. J. (2006) Epithelial-mesenchymal interactions in pulmonary fibrosis. *Semin. Respir. Crit. Care Med.* **27**, 600–612
9. Borok, Z. (2014) Alveolar epithelium: beyond the barrier. *Am. J. Respir. Cell Mol. Biol.* **50**, 853–856
10. Willis, B. C., Liebler, J. M., Luby-Phelps, K., Nicholson, A. G., Crandall, E. D., du Bois, R. M., and Borok, Z. (2005) Induction of epithelial-mesenchymal transition in alveolar epithelial cells by transforming growth factor-beta1: potential role in idiopathic pulmonary fibrosis. *Am. J. Pathol.* **166**, 1321–1332
11. Chapman, H. A. (2011) Epithelial-mesenchymal interactions in pulmonary fibrosis. *Annu. Rev. Physiol.* **73**, 413–435
12. Kim, K. K., Kugler, M. C., Wolters, P. J., Robillard, L., Galvez, M. G., Brumwell, A. N., Sheppard, D., and Chapman, H. A. (2006) Alveolar epithelial cell mesenchymal transition develops in vivo during pulmonary fibrosis and is regulated by the extracellular matrix. *Proc. Natl. Acad. Sci. USA* **103**, 13180–13185
13. Kim, K. K., Wei, Y., Szekeres, C., Kugler, M. C., Wolters, P. J., Hill, M. L., Frank, J. A., Brumwell, A. N., Wheeler, S. E., Kreidberg, J. A., and Chapman, H. A. (2009) Epithelial cell alpha3beta1 integrin links beta-catenin and Smad signaling to promote myofibroblast formation and pulmonary fibrosis. *J. Clin. Invest.* **119**, 213–224
14. Tanjore, H., Xu, X. C., Polosukhin, V. V., Degryse, A. L., Li, B., Han, W., Sherrill, T. P., Plieth, D., Neilson, E. G., Blackwell, T. S., and Lawson, W. E. (2009) Contribution of epithelial-derived fibroblasts to bleomycin-induced lung fibrosis. *Am. J. Respir. Crit. Care Med.* **180**, 657–665
15. Degryse, A. L., Tanjore, H., Xu, X. C., Polosukhin, V. V., Jones, B. R., McMahon, F. B., Gleaves, L. A., Blackwell, T. S., and Lawson, W. E. (2010) Repetitive intratracheal bleomycin models several features of idiopathic pulmonary fibrosis. *Am. J. Physiol. Lung Cell. Mol. Physiol.* **299**, L442–L452
16. Saito, F., Tasaka, S., Inoue, K., Miyamoto, K., Nakano, Y., Ogawa, Y., Yamada, W., Shiraishi, Y., Hasegawa, N., Fujishima, S., Takano, H., and Ishizaka, A. (2008) Role of interleukin-6 in bleomycin-induced lung inflammatory changes in mice. *Am. J. Respir. Cell Mol. Biol.* **38**, 566–571
17. Pedroza, M., Schneider, D. J., Karmouty-Quintana, H., Coote, J., Shaw, S., Corrigan, R., Molina, J. G., Alcorn, J. L., Galas, D., Gelinas, R., and Blackburn, M. R. (2011) Interleukin-6 contributes to inflammation and remodeling in a model of adenosine mediated lung injury. *PLoS One* **6**, e22667
18. Le, T. T., Karmouty-Quintana, H., Melicoff, E., Weng, T., Chen, N. Y., Pedroza, M., Zhou, Y., Davies, J., Philip, K., Molina, J., Luo, F., George, A. T., Garcia-Morales, L. J., Bunge, R. R., Bruckner, B. A., Loebe, M., Seethamraju, H., Agarwal, S. K., and Blackburn, M. R. (2014) Blockade of IL-6 trans signaling attenuates pulmonary fibrosis. *J. Immunol.* **193**, 3755–3768
19. Gourh, P., Arnett, F. C., Assassi, S., Tan, F. K., Huang, M., Diekman, L., Mayes, M. D., Reveille, J. D., and Agarwal, S. K. (2009) Plasma cytokine profiles in systemic sclerosis: associations with autoantibody subsets and clinical manifestations. *Arthritis Res. Ther.* **11**, R147
20. Zhou, Y., Murthy, J. N., Zeng, D., Belardinelli, L., and Blackburn, M. R. (2010) Alterations in adenosine metabolism and signaling in patients with chronic obstructive pulmonary disease and idiopathic pulmonary fibrosis. *PLoS One* **5**, e9224
21. Shigekawa, M., Takehara, T., Kodama, T., Hikita, H., Shimizu, S., Li, W., Miyagi, T., Hosui, A., Tatsumi, T., Ishida, H., Kanto, T., Hiramatsu, N., and Hayashi, N. (2011) Involvement of STAT3-regulated hepatic soluble factors in attenuation of stellate cell activity and liver fibrogenesis in mice. *Biochem. Biophys. Res. Commun.* **406**, 614–620
22. Deng, P., Wang, C., Chen, L., Wang, C., Du, Y., Yan, X., Chen, M., Yang, G., and He, G. (2013) Sesamin induces cell cycle arrest and apoptosis through the inhibition of signal transducer

and activator of transcription 3 signalling in human hepatocellular carcinoma cell line HepG2. *Biol. Pharm. Bull.* **36**, 1540–1548
23. Xu, C. P., Li, X., Hu, Y. J., Cui, Z., Wang, L., Liang, L., Zhou, Y. L., Yang, Y. J., and Yu, B. (2015) Quantitative proteomics reveals ELP2 as a regulator to the inhibitory effect of TNF-α on osteoblast differentiation. *J. Proteomics* **114**, 234–246
24. Mair, M., Zollner, G., Schneller, D., Musteanu, M., Fickert, P., Gumhold, J., Schuster, C., Fuchsbichler, A., Bilban, M., Tauber, S., Esterbauer, H., Kenner, L., Poli, V., Blaas, L., Kornfeld, J. W., Casanova, E., Mikulits, W., Trauner, M., and Eferl, R. (2010) Signal transducer and activator of transcription 3 protects from liver injury and fibrosis in a mouse model of sclerosing cholangitis. *Gastroenterology* **138**, 2499–2508
25. Ogata, H., Chinen, T., Yoshida, T., Kinjyo, I., Takaesu, G., Shiraishi, H., Iida, M., Kobayashi, T., and Yoshimura, A. (2006) Loss of SOCS3 in the liver promotes fibrosis by enhancing STAT3-mediated TGF-beta1 production. *Oncogene* **25**, 2520–2530
26. Dai, B., Cui, M., Zhu, M., Su, W. L., Qiu, M. C., and Zhang, H. (2013) STAT1/3 and ERK1/2 synergistically regulate cardiac fibrosis induced by high glucose. Cell. Physiol. Biochem. **32**, 960–971
27. Moodley, Y. P., Scaffidi, A. K., Misso, N. L., Keerthisingam, C., McAnulty, R. J., Laurent, G. J., Mutsaers, S. E., Thompson, P. J., and Knight, D. A. (2003) Fibroblasts isolated from normal lungs and those with idiopathic pulmonary fibrosis differ in interleukin-6/gp130-mediated cell signaling and proliferation. *Am. J. Pathol.* **163**, 345–354
28. Pechkovsky, D. V., Prêle, C. M., Wong, J., Hogaboam, C. M., McAnulty, R. J., Laurent, G. J., Zhang, S. S., Selman, M., Mutsaers, S. E., and Knight, D. A. (2012) STAT3-mediated signaling dysregulates lung fibroblast-myofibroblast activation and differentiation in UIP/IPF. *Am. J. Pathol.* **180**, 1398–1412
29. O'Donoghue, R. J., Knight, D. A., Richards, C. D., Prêle, C. M., Lau, H. L., Jarnicki, A. G., Jones, J., Bozinovski, S., Vlahos, R., Thiem, S., McKenzie, B. S., Wang, B., Stumbles, P., Laurent, G. J., McAnulty, R. J., Rose-John, S., Zhu, H. J., Anderson, G. P., Ernst, M. R., and Mutsaers, S. E. (2012) Genetic partitioning of interleukin-6 signalling in mice dissociates Stat3 from Smad3-mediated lung fibrosis. *EMBO Mol. Med.* **4**, 939–951
30. Dong, Z., Lu, X., Yang, Y., Zhang, T., Li, Y., Chai, Y., Lei, W., Li, C., Ai, L., and Tai, W. (2015) IL-27 alleviates the bleomycin-induced pulmonary fibrosis by regulating the Th17 cell differentiation. *BMC Pulm. Med.* **15**, 13
31. García-Prieto, E., González-López, A., Cabrera, S., Astudillo, A., Gutiérrez-Fernández, A., Fanjul-Fernandez, M., Batalla-Solís, E., Puente, X. S., Fueyo, A., López-Otín, C., and Albaiceta, G. M. (2010) Resistance to bleomycin-induced lung fibrosis in MMP-8 deficient mice is mediated by interleukin-10. *PLoS One* **5**, e13242
32. Ataie-Kachoie, P., Pourgholami, M. H., Richardson, D. R., and Morris, D. L. (2014) Gene of the month: interleukin 6 (IL-6). *J. Clin. Pathol.* **67**, 932–937
33. Ma, X., Chen, R., Liu, X., Xie, J., Si, K., and Duan, L. (2013) Effects of matrine on JAK-STAT signaling transduction pathways in bleomycin-induced pulmonary fibrosis. *Afr. J. Tradit. Complement. Altern. Med.* **10**, 442–448
34. Zhou, X., Li, Y. J., Gao, S. Y., Wang, X. Z., Wang, P. Y., Yan, Y. F., Xie, S. Y., and Lv, C. J. (2015) Sulindac has strong antifibrotic effects by suppressing STAT3-related miR-21. *J. Cell. Mol. Med.* **19**, 1103–1113
35. Gao, S. Y., Zhou, X., Li, Y. J., Liu, W. L., Wang, P. Y., Pang, M., Xie, S. Y., and Lv, C. J. (2014) Arsenic trioxide prevents rat pulmonary fibrosis via miR-98 overexpression. *Life Sci.* **114**, 20–28
36. Xu, X., Kasembeli, M. M., Jiang, X., Tweardy, B. J., and Tweardy, D. J. (2009) Chemical probes that competitively and selectively inhibit Stat3 activation. *PLoS One* **4**, e4783
37. Dave, B., Landis, M. D., Tweardy, D. J., Chang, J. C., Dobrolecki, L. E., Wu, M. F., Zhang, X., Westbrook, T. F., Hilsenbeck, S. G., Liu, D., and Lewis, M. T. (2012) Selective small molecule Stat3 inhibitor reduces breast cancer tumor-initiating cells and improves recurrence free survival in a human-xenograft model. *PLoS One* **7**, e30207
38. Redell, M. S., Ruiz, M. J., Alonzo, T. A., Gerbing, R. B., and Tweardy, D. J. (2011) Stat3 signaling in acute myeloid leukemia: ligand-dependent and -independent activation and induction of apoptosis by a novel small-molecule Stat3 inhibitor. *Blood* **117**, 5701–5709
39. Zhang, L., Pan, J., Dong, Y., Tweardy, D. J., Dong, Y., Garibotto, G., and Mitch, W. E. (2013) Stat3 activation links a C/EBPδ to myostatin pathway to stimulate loss of muscle mass. *Cell Metab.* **18**, 368–379
40. Pinart, M., Serrano-Mollar, A., Llatjós, R., Rocco, P. R., and Romero, P. V. (2009) Single and repeated bleomycin intratracheal instillations lead to different biomechanical changes in lung tissue. *Respir. Physiol. Neurobiol.* **166**, 41–46
41. Ashcroft, T., Simpson, J. M., and Timbrell, V. (1988) Simple method of estimating severity of pulmonary fibrosis on a numerical scale. *J. Clin. Pathol.* **41**, 467–470
42. Hübner, R. H., Gitter, W., El Mokhtari, N. E., Mathiak, M., Both, M., Bolte, H., Freitag-Wolf, S., and Bewig, B. (2008) Standardized quantification of pulmonary fibrosis in histological samples. *Biotechniques* **44**, 507–511
43. Corti, M., Brody, A. R., and Harrison, J. H. (1996) Isolation and primary culture of murine alveolar type II cells. *Am. J. Respir. Cell Mol. Biol.* **14**, 309–315
44. Seluanov, A., Vaidya, A., and Gorbunova, V. (2010) Establishing primary adult fibroblast cultures from rodents. *J. Vis. Exp.* (44): 2033
45. Ueno, M., Maeno, T., Nomura, M., Aoyagi-Ikeda, K., Matsui, H., Hara, K., Tanaka, T., Iso, T., Suga, T., and Kurabayashi, M. (2011) Hypoxia-inducible factor-1α mediates TGF-β-induced PAI-1 production in alveolar macrophages in pulmonary fibrosis. *Am. J. Physiol. Lung Cell. Mol. Physiol.* **300**, L740–L752
46. Eitzman, D. T., McCoy, R. D., Zheng, X., Fay, W. P., Shen, T., Ginsburg, D., and Simon, R. H. (1996) Bleomycin-induced pulmonary fibrosis in transgenic mice that either lack or overexpress the murine plasminogen activator inhibitor-1 gene. *J. Clin. Invest.* **97**, 232–237
47. Tanaka, K., Tanaka, Y., Namba, T., Azuma, A., and Mizushima, T. (2010) Heat shock protein 70 protects against bleomycin-induced pulmonary fibrosis in mice. *Biochem. Pharmacol.* **80**, 920–931
48. Heinrich, P. C., Behrmann, I., Müller-Newen, G., Schaper, F., and Graeve, L. (1998) Interleukin-6-type cytokine signalling through the gp130/Jak/STAT pathway. *Biochem. J.* **334**, 297–314
49. Heinrich, P. C., Behrmann, I., Haan, S., Hermanns, H. M., Müller-Newen, G., and Schaper, F. (2003) Principles of interleukin (IL)-6-type cytokine signalling and its regulation. *Biochem. J.* **374**, 1–20
50. Kishimoto, T., Akira, S., Narazaki, M., and Taga, T. (1995) Interleukin-6 family of cytokines and gp130. *Blood* **86**, 1243–1254
51. Levy, D. E., and Darnell, Jr., J. E. (2002) Stats: transcriptional control and biological impact. *Nat. Rev. Mol. Cell Biol.* **3**, 651–662
52. Zhong, H., Belardinelli, L., Maa, T., and Zeng, D. (2005) Synergy between A2B adenosine receptors and hypoxia in activating human lung fibroblasts. *Am. J. Respir. Cell Mol. Biol.* **32**, 2–8.
53. Mozaffarian, A., Brewer, A. W., Trueblood, E. S., Luzina, I. G., Todd, N. W., Atamas, S. P., and Arnett, H. A. (2008) Mechanisms of oncostatin M-induced pulmonary inflammation and fibrosis. *J. Immunol.* **181**, 7243–7253
54. Tang, W., Geba, G. P., Zheng, T., Ray, P., Homer, R. J., Kuhn III, C., Flavell, R. A., and Elias, J. A. (1996) Targeted expression of IL-11 in the murine airway causes lymphocytic inflammation, bronchial remodeling, and airways obstruction. *J. Clin. Invest.* **98**, 2845–2853
55. Kasembeli, M. M., Xu, X., and Tweardy, D. J. (2009) SH2 domain binding to phosphopeptide ligands: potential for drug targeting. *Front. Biosci. (Landmark Ed.)* **14**, 1010–1022
56. Baran, C. P., Opalek, J. M., McMaken, S., Newland, C. A., O'Brien, Jr., J. M., Hunter, M. G., Bringardner, B. D., Monick, M. M., Brigstock, D. R., Stromberg, P. C., Hunninghake, G. W., and Marsh, C. B. (2007) Important roles for macrophage colony-stimulating factor, CC chemokine ligand 2, and mononuclear phagocytes in the pathogenesis of pulmonary fibrosis. *Am. J. Respir. Crit. Care Med.* **176**, 78–89
57. Moeller, A., Ask, K., Warburton, D., Gauldie, J., and Kolb, M. (2008) The bleomycin animal model: a useful tool to investigate treatment options for idiopathic pulmonary fibrosis? *Int. J. Biochem. Cell Biol.* **40**, 362–382

58. Tzouvelekis, A., Harokopos, V., Paparountas, T., Oikonomou, N., Chatziioannou, A., Vilaras, G., Tsiambas, E., Karameris, A., Bouros, D., and Aidinis, V. (2007) Comparative expression profiling in pulmonary fibrosis suggests a role of hypoxia-inducible factor-1alpha in disease pathogenesis. *Am. J. Respir. Crit. Care Med.* **176**, 1108–1119
59. Hattori, N., Degen, J. L., Sisson, T. H., Liu, H., Moore, B. B., Pandrangi, R. G., Simon, R. H., and Drew, A. F. (2000) Bleomycin-induced pulmonary fibrosis in fibrinogen-null mice. *J. Clin. Invest.* **106**, 1341–1350
60. Namba, T., Tanaka, K., Hoshino, T., Azuma, A., and Mizushima, T. (2011) Suppression of expression of heat shock protein 70 by gefitinib and its contribution to pulmonary fibrosis. *PLoS One* **6**, e27296
61. Schneider, D. J., Wu, M., Le, T. T., Cho, S. H., Brenner, M. B., Blackburn, M. R., and Agarwal, S. K. (2012) Cadherin-11 contributes to pulmonary fibrosis: potential role in TGF-beta production and epithelial to mesenchymal transition. FASEB J. **26**, 503–512
62. Liu, Y., Liu, H., Meyer, C., Li, J., Nadalin, S., Königsrainer, A., Weng, H., Dooley, S., and ten Dijke, P. (2013) Transforming growth factor-β (TGF-β)-mediated connective tissue growth factor (CTGF) expression in hepatic stellate cells requires Stat3 signaling activation. *J. Biol. Chem.* **288**, 30708–30719
63. Becker, C., Fantini, M. C., Schramm, C., Lehr, H. A., Wirtz, S., Nikolaev, A., Burg, J., Strand, S., Kiesslich, R., Huber, S., Ito, H., Nishimoto, N., Yoshizaki, K., Kishimoto, T., Galle, P. R., Blessing, M., Rose-John, S., and Neurath, M. F. (2004) TGF-beta suppresses tumor progression in colon cancer by inhibition of IL-6 trans-signaling. *Immunity* **21**, 491–501
64. Jenkins, B. J., Grail, D., Nheu, T., Najdovska, M., Wang, B., Waring, P., Inglese, M., McLoughlin, R. M., Jones, S. A., Topley, N., Baumann, H., Judd, L. M., Giraud, A. S., Boussioutas, A., Zhu, H. J., and Ernst, M. (2005) Hyperactivation of Stat3 in gp130 mutant mice promotes gastric hyperproliferation and desensitizes TGF-beta signaling. *Nat. Med.* **11**, 845–852
65. Yamamoto, T., Matsuda, T., Muraguchi, A., Miyazono, K., and Kawabata, M. (2001) Cross-talk between IL-6 and TGF-beta signaling in hepatoma cells. *FEBS Lett.* **492**, 247–253
66. Elias, J. A., Lentz, V., and Cummings, P. J. (1991) Transforming growth factor-beta regulation of IL-6 production by unstimulated and IL-1-stimulated human fibroblasts. *J. Immunol.* **146**, 3437–3443
67. Rochester, C. L., Ackerman, S. J., Zheng, T., and Elias, J. A. (1996) Eosinophil-fibroblast interactions. Granule major basic protein interacts with IL-1 and transforming growth factor-beta in the stimulation of lung fibroblast IL-6-type cytokine production. *J. Immunol.* **156**, 4449–4456

*Received for publication April 6, 2015.*
*Accepted for publication August 17, 2015.*